Effects of contemporary shifts of range margins on patterns of genetic structure and mating system in two coastal plant species

Mathilde Latron, Jean-François Arnaud, Héloïse Ferla, Cécile Godé, Anne Duputié

Effects of contemporary shifts of range margins on patterns of genetic structure and mating system in two coastal plant species

Mathilde Latron, Jean-François Arnaud, Héloïse Ferla, Cécile Godé, & Anne Duputié*

Univ. Lille, CNRS, UMR 8198 – Evo-Eco-Paleo, F-59000 Lille, France
* Corresponding author
E-mail: anne.duputie@univ-lille.fr

Abstract

Species' geographical ranges are often restricted due to niche limitation resulting in geographical isolation and reduced population size at range margins. Under the 'abundant center' paradigm, static marginal populations are thus expected to show higher genetic differentiation and lower genetic diversity than core populations. Low mate availability may also drive shifts towards higher propensity for selfing in geographically marginal populations. However, these predictions remain to be validated for contemporary range shifts occurring under current environmental change. This study is devoted to bridging this gap and assesses the spatial patterns of genetic structure and mating system across the geographical range of two coastal plant species characterized by contrasting contemporary range dynamics: the receding myrmecochorous Dune pansy (*Viola tricolor* subsp. *curtisii*) and the widespread expanding hydrochorous Rock samphire (*Crithmum maritimum*). Both species exhibited high propensity for selfing, with indications of inbreeding depression acting at early life stages. In Dune pansy, a biogeographical break was observed between core and marginal populations, with trailing-edge populations showing higher levels of genetic differentiation, reduced genetic diversity and higher levels of selfing estimated through progeny arrays. In contrast, genetic structuring was weak in Rock samphire and no clear spatial trends were observed in genetic diversity nor in mating system, likely the result of efficient long-distance seed dispersal by sea-surface currents. Our study highlights that key species differences in life-history traits related to dispersal and/or mate limitation modify the expectations of genetic diversity loss and mating system shift in contemporary range-expanding populations, as compared to historical core populations.

Keywords

expanding and contracting range edges; genetic differentiation; genetic diversity; mating system; peripheral populations; range limit

Introduction

Numerous ecological and evolutionary processes shape the geographical distribution of species, including climate features, the strength of biotic interactions, habitat and resource availability, anthropogenic habitat modifications, and key life-history traits such as mating system variation or dispersal abilities (Gaston, 2009; Eckert *et al.*, 2010; Grossenbacher *et al.*, 2015; Moeller *et al.*, 2017). Static species' range boundaries often stem from declining environmental suitability with increasing distance from the species' range core (e.g. Jump *et al.*, 2003). Under the 'abundant center' paradigm, static equilibrium range limits might take place, with marginal populations prone to extinction events or bottlenecks, as they occur in less suitable habitats with low density of conspecifics (Brown, 1984; Sagarin *et al.*, 2006; Phillips *et al.*, 2010). Over the past decades, many empirical studies indeed showed increased genetic drift, shifts in mating system, and potentially reduced adaptive potential in marginal populations as compared to core populations (Eckert *et al.*, 2008). These studies often involved surveys of historical range shifts since the ice retreat of last glacial maximum or rapidly expanding invasive species (e.g. Hewitt, 2000; Hampe and Petit, 2005; Colautti *et al.*, 2010; Leys *et al.*, 2014; Hopper *et al.*, 2019). Nonetheless, ongoing human-driven environmental changes trigger current geographical expansion or retraction of species' geographical ranges and local adaptation to changing conditions through the evolution of key life-history traits related to dispersal and reproductive traits (Jump and Peñuelas, 2005; Colautti *et*

al., 2010; e.g. Steinbauer *et al.*, 2018; Vilà-Cabrera *et al.*, 2019). In this respect, empirical evidence of concomitant changes in mating system and patterns of genetic structure for contemporary shifting ranges in a changing world is still lacking, especially in sessile organisms such as plant species for which gene flow within and among populations only occurs through seed and pollen dispersal (Hargreaves and Eckert, 2014; Auffret *et al.*, 2017). This study aims at bridging this gap and focuses on spatial patterns of genetic structure and mating system across two plant species' geographical ranges characterized by ongoing contrasting dynamics of expansion and contraction.

Understanding the spatial genetic structure across species' ranges using core populations and expanding or contracting range populations is motivated by evolutionary and management/conservation concerns (Vilà-Cabrera *et al.*, 2019). Populations located at range margins are indeed generally geographically isolated within a matrix of inhospitable habitats and often of low population size (Kawecki, 2008). When compared to core populations, the levels of genetic diversity are expected to be lower in marginal populations because of magnified genetic drift effects through reduced effective population size and founder effects (e.g. Hewitt 2000; Lönn & Prentice 2002; Leys *et al.* 2014; reviewed in Eckert *et al.* 2008). At the same time, an increase in among-population genetic differentiation is also expected owing to reduced levels of gene flow at range margins compared with core populations (e.g. Griffin and Willi, 2014; Samis *et al.*, 2016). Although both types of effects on genetic structure are supported by a large body of empirical work for static range boundaries (Eckert *et al.*, 2008; López-Villalobos and Eckert, 2018), differences in genetic structure between core and currently expanding or receding marginal populations still need to be investigated.

Theoretical studies showed that, in addition to drift and founder effects, ongoing extinction and recolonization processes are also an important determinant of genetic structure (Slatkin, 1977; Whitlock and McCauley, 1990). At range margins, the turnover of local populations can enhance opportunities for both genetic drift and gene flow, depending on the number of colonists relative to the number of recurrent migrants, and on whether the colonists arise from a single source (propagule-pool model) or many sources (migrant-pool model, see Pannell & Charlesworth 2000 for review). Therefore, counterintuitive patterns of genetic structure may arise for contemporary range shifts. First, marginal populations may be larger and more genetically diverse than core populations if the geographical range of the species is not constrained by habitat suitability (Sagarin *et al.*, 2006; Eckert *et al.*, 2008). Second, whereas lower levels of genetic diversity are expected in leading-edge populations, higher genetic diversity may persist in remnant trailing-edge populations (Hampe and Petit, 2005; Arenas *et al.*, 2012; Vilà-Cabrera *et al.*, 2019). Third, asymmetrical long-distance dispersal may increase the levels of genetic diversity at the leading edge of the distribution and lower the among-population genetic differentiation (Bialozyt *et al.*, 2006; Eckert *et al.*, 2008; Leys *et al.*, 2014). Overall, population genetic differentiation can increase or decrease depending on the source of colonists, the rate of colonization and the rate of gene flow among static marginal populations (Whitlock and McCauley, 1990; Le Corre and Kremer, 1998; Pannell and Charlesworth, 2000). These patterns remain to be investigated in native species for which geographical ranges are currently shifting.

Mating system variation can also play a role in successful colonization of marginal habitats characterized by low densities of conspecifics and/or poor pollination opportunities (Jain, 1976; Grossenbacher *et al.*, 2015; Pannell, 2015; Moeller *et al.*, 2017). Provided that inbreeding depression is low and/or mildly deleterious alleles are purged, self-fertilization is thought to facilitate geographic expansion (Baker, 1955; Pannell, 2015). Theoretical models predict that populations located at range margins should evolve towards selfing (Pannell and Barrett, 1998; Cheptou and Massol, 2009; Rodger *et al.*, 2018), and many empirical studies suggest that the propensity for selfing is higher in leading-edge populations (Darling *et al.*, 2008; Griffin and Willi, 2014; López-Villalobos and Eckert, 2018; see however Herlihy and Eckert, 2005; Colautti *et al.*, 2010). In trailing-edge populations, mate limitation may also select for higher selfing rates, which may be detrimental for long-term species' persistence in a warming world due to increased genetic drift and resulting depletion in adaptive standing genetic variation (Hampe and Petit, 2005; Levin, 2012; Hargreaves and Eckert, 2014; Vilà-Cabrera *et al.*, 2019).

Broadly speaking, newly established populations at expanding leading edges are expected to show low effective population sizes and moderate levels of genetic diversity, high selfing rates, and possibly low incoming gene flow through long-distance dispersal events relative to core populations. On the other hand, trailing-edge populations are expected to face habitat fragmentation, triggering high genetic differentiation among populations. However, these predictions mostly hold for historical range shifts that left

genetic footprint of postglacial recolonization or retraction. Empirical support of concomitant changes in mating system and genetic structure for ongoing contracting and expanding ranges are still lacking (Hargreaves and Eckert, 2014).

To bridge these gaps, we analyzed the genetic structure and mating system of two diploid native plant species with contrasting life-history traits: the widespread Rock samphire (*Crithmum maritimum*, Apiaceae), currently expanding in northwestern Europe, and the endangered Dune pansy (*Viola tricolor* subsp *curtisii,* Violaceae) which is receding in northern France (Figure 1). Both species are perennial and self-compatible and have a strictly coastal distribution, which facilitates categorization into central (core) and marginal populations. These two focal species differ in life-history traits, notably in seed dispersal mode (hydrochory and likely associated long-distance dispersal events through marine currents for Rock samphire, short-distance dispersal events through myrmecochory for Dune pansy). We investigated the large-scale spatial patterns of genetic structure of a comprehensive sampling of populations collected from the range center to the leading (Rock samphire) or trailing edge (Dune pansy) of their geographical distribution. We specifically addressed the following questions related to contemporary expanding or receding geographical ranges:

1. Do currently shifting marginal populations display lower census and effective population size? If so, are they more genetically depauperate than stable historical core populations? If so, are they more genetically depauperate than core populations? We expect low genetic diversity in expanding colonizing populations of Rock samphire. However, a genetic legacy of high genetic diversity at the contemporary trailing edge of the species' range could be expected for the retracting populations of Dune pansy.
2. Do expanding or retracting populations show higher levels of genetic differentiation compared with stable historical core populations and if so, to what extent? In spite of the mitigating effect of long-distance dispersal events through hydrochory, we expect stronger levels of genetic differentiation for Rock samphire populations at expanding range margins due to sequential founder effects. We also expect that biogeographical legacy should attenuate this pattern among currently shifting trailing-edge populations of Dune pansy.
3. Can we detect fine-scale genetic discontinuities mirroring contemporary expansion and retraction shifts? We expect

asymmetrical gene flow from core (source) to contemporary expanding or retracting populations (sinks).
4. Is there a shift towards a higher propensity for selfing in marginal populations of currently shifting species, as predicted by Baker's law for stable historical range limits? We predict no significant changes in selfing rates for these species, owing to the time-lag necessary to approach genetic equilibrium (Pannell, 2015).

METHODS
Study species, sampling and genotyping

Rock samphire (*Crithmum maritimum* L., Apiaceae) is an insect-pollinated perennial halophyte and heliophilous coastal plant found on rocky shores in Western Europe (Figure 1A). The species is restricted to a thin strip along the shoreline, and produces small corky achenes which can drift through marine currents, with seeds remaining viable over several months (Ridley, 1930). Self-fertilization occurs, but strictly requires a pollination vector (Latron *et al*. unpublished results). Patterns of within-population gene flow in Rock samphire may mostly occur over short spatial distance through barochory and through pollen dispersal owing to local pollinator foraging. For the past decades, its geographical distribution has been expanding northwards in man-made habitats along the coastlines of northern France, Belgium and the Netherlands, most often on the south-facing parts of dikes, pontoons, pilings, riprap and other artificial structures (Lambinon and Verloove, 2012). Sampling included populations from the core of the range, on the Atlantic coast, up to the leading edge of the species distribution in the Netherlands (Figure 1A).

Dune pansy (*Viola tricolor* subsp*. curtisii* [E.Forst] Syme, Violaceae) is an endangered insect-pollinated perennial species commonly found on semi-stabilized sand-dunes on the coasts of the English Channel and North Sea (Figure 1B). As for Rock samphire, self-fertilization obligately requires a pollinator (Latron *et al*. unpublished results). Determinants of among-population dispersal events are not documented in Dune pansy: seeds are mostly dispersed over very short distances, a few meters generally, by myrmecochory (Warren *et al.*, 2010; Rix, 2014). Over the past decades, Dune pansy lost habitats in northern France, due to urbanization and to dune fixation in peri-urban areas, and is now protected. We thus sampled populations of Dune pansy from the trailing edge of its distribution in northern France, to more central populations located in the Netherlands (Figure 1B).
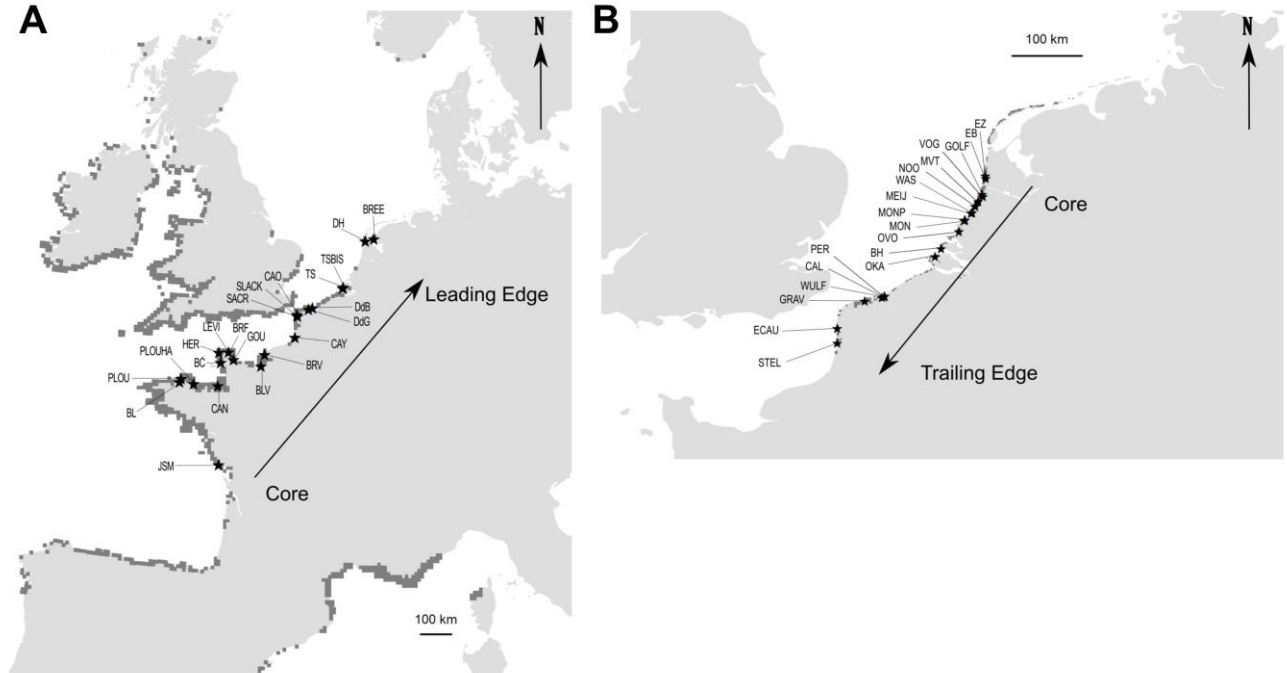
Figure 1: Species' geographical distribution (grey squares) and geographical locations of sampled populations (black stars) for *Crithmum maritimum* (A) and *Viola tricolor* subsp. *curtisii* (B). Sources of distribution data: http://siflore.fcbn.fr and http://www.gbif.org/.

Rock samphire is a widespread species located around the Mediterranean and Atlantic coasts, up to the British Islands. Rock samphire sampling only covered the western part of continental Atlantic coast, excluding the UK (Figure 1A). Dune pansy sampling covered the southern part of the species' geographical distribution (Figure 1B). For both species, we sampled marginal populations as exhaustively as possible, by screening every accessible habitat near range edges, while we collected well-distributed populations in the center of their distribution ranges (Figure 1; Tables 1 and 2). In the core of each species' distribution, populations occurred at almost every site with suitable habitat. Towards the edge of the distribution, the number of suitable habitats declines, fewer are occupied and populations tend to be smaller. For Rock samphire, sampling was almost exhaustive from Den Helder (DH) to Breezanddijk (BREE; the Netherlands), and scattered in the more southern parts of the distribution range. For Dune pansy, population sampling was exhaustive from Stella-Plage (STEL) to Gravelines (GRAV, France), and scattered in the more northern parts of its geographic distribution. We also assessed the number of individuals in each population to get a census population size (Tables 1 and 2).

Overall, we sampled 22 Rock samphire populations and 19 Dune pansy populations, with sampling size varying from 3 to 39 individuals (24.3 ± 11.1) and from 23 to 30 individuals (29.6 ± 1.6), for a total of 508 and 563 fresh leaf samples, respectively (Figure 1, Tables 1 and 2). WGS 84 coordinates of each individual were recorded. Coastal geographical distances among populations were calculated on the basis of the southernmost core population for Rock samphire (JSM) and the northernmost core population for Dune pansy (EZ).

Leaves were dried for 3 days at 50°C, then DNA was extracted with the NucleoSpin 96 Plant II kit (Macherey Nagel, Duren, Germany) according to the manufacturer's recommendations. All sampled individuals were genotyped at 21 and 10 nuclear microsatellite loci (Table S1) for Rock samphire and Dune pansy, respectively, as described in Latron *et al.* (2018). PCR products were sized using an ABI PRISM 3130 Sequencer and the software GENEMAPPER version 5 (Applied Biosystems). All genotypes were independently checked by two operators. Amplification failure was scarce (0.4% for Rock samphire and 0.9% for Dune pansy).

Table 1*:* Summary statistics of genetic diversity, selfing rates, and fine-scale spatial genetic structure in *Crithmum maritimum,* based on 21 nuclear microsatellite loci. Populations are listed from southern (core) populations to northern (leading-edge) populations. Pop: Population name; N: sample size, A_r: allelic richness; H_O: observed heterozygosity; H_E: genetic diversity; F_{IS}: intrapopulation fixation index; *HL:* homozygosity by locus; sF_{IS}: selfing rates based on F_{IS}; sID: selfing rates based on identity disequilibrium; sPA: selfing rate estimated from progeny-array analyses (SD < 0.001 for all populations); *Sp*: strength of spatial genetic structure; N_e: effective population size; census size: field estimate of population census size. *: $p<0.05$, **: $p<0.01$, ***: $p<0.001$.

Pop	Location	Lat	Lon	N	A_r	H_O	H_E	F_{IS}	HL	sF_{IS}	sID	sPA	*Sp*	N_e	Census size
JSM	Jard-sur-Mer	46.41	-1.61	19	2.47	0.19	0.32	0.40***	0.73	0.57	0.35	-	-0.003	20	≥ 100
BL	Phare de Beg Leguer	48.74	-3.55	20	1.85	0.23	0.27	0.14*	0.68	0.25	0.15	0.80	0.005	22	≥ 300
PLOU	Ploumanac'h	48.83	-3.49	20	2.00	0.07	0.24	0.72***	0.90	0.84	0.89	-	0.152**	-	≥ 100
PLOUHA	Plouha	48.71	-2.92	11	1.66	0.15	0.18	0.17	0.77	0.28	0.08	-	0.03	2	≥ 500
CAN	Cancale	48.70	-1.85	20	1.52	0.09	0.13	0.32***	0.87	0.48	0.77	0.72	0.048**	-	≥ 50
BC	Barneville-Carteret	49.37	-1.80	25	1.14	0.03	0.04	0.32*	0.96	0.48	-	-	-0.006	-	≥ 300
HER	Herqueville	49.66	-1.88	36	2.14	0.25	0.35	0.30***	0.66	0.47	0.47	-	0.070***	4	≥ 2000
LEVI	Cap Levi	49.70	-1.47	35	2.22	0.21	0.31	0.34***	0.69	0.51	0.31	-	0.043***	22	≥ 1000
BRF	Barfleur	49.67	-1.26	35	2.50	0.21	0.34	0.39***	0.71	0.56	0.40	-	0.017**	47	≥ 500
GOU	Les Gougins	49.49	-1.26	35	2.34	0.13	0.33	0.61***	0.82	0.76	0.82	-	0.062***	4	≥ 300
BLV	Blonville-sur-Mer	49.34	0.03	26	1.78	0.02	0.19	0.88***	0.97	0.93	0.94	-	0.224***	-	≥ 50
BRV	Bruneval	49.66	0.16	38	1.38	0.05	0.09	0.46***	0.93	0.63	0.53	-	0.111***	6	≥ 100
CAY	Cayeux	50.19	1.50	16	1.33	0.08	0.1	0.24*	0.90	0.38	0.44	-	0.036	11	≥ 300
SACR	Ambleteuse, Slack estuary	50.81	1.60	20	2.68	0.22	0.36	0.39***	0.68	0.56	0.58	-	0.004	18	≥ 50
SLACK	Ambleteuse, beach	50.80	1.60	23	2.32	0.21	0.31	0.33***	0.70	0.50	0.47	0.84	0.040**	6	≥ 100
CAO	Cran aux Oeufs	50.85	1.58	19	1.11	0.02	0.03	0.46*	1.00	0.63	0.72	-	0.079	-	≥ 100
DdG	Digue de Gravelines	51.01	2.10	4	-	-	-	-	-	-	-	-	-	-	4
DdB	Digue du Braek	51.05	2.29	22	2.05	0.16	0.3	0.47***	0.76	0.64	0.54	0.79	0.115***	2	≥ 300
TS	Topshuis south	51.62	3.69	39	1.69	0.05	0.18	0.74***	0.94	0.85	0.92	0.88	0.170***	-	≥ 60
TSBIS	Topshuis North	51.64	3.71	35	1.38	0.13	0.15	0.17**	0.86	0.29	0.25	-	0	13	35
DH	Den Helder	52.96	4.78	14	1.68	0.11	0.23	0.53***	0.88	0.69	-	1.00	0.216**	-	≥ 30
BREE	Breezanddijk	53.02	5.20	3	-	-	-	-	-	-	-	-	-	-	3

Table 2: Summary statistics of genetic diversity, selfing rates, and fine-scale spatial genetic structure in *Viola curtisii* subsp. *curtisii,* based on 10 nuclear microsatellite loci. Populations are listed from northern (core) populations to southern (trailing-edge) populations Pop: Population name; N: sample size, A_r: allelic richness; H_O: observed heterozygosity; H_E: genetic diversity; F_{IS}: intrapopulation fixation index; HL: homozygosity by locus; sF_{IS}: selfing rates based on F_{IS}; sID: selfing rates based on identity disequilibrium; sPA: selfing rate estimated from progeny-array analyses (SD < 0.002 for all populations); Sp: strength of spatial genetic structure; N_e: effective population size; census size: field estimate of population census size. *: $p < 0.05$, **: $p < 0.01$, ***: $p < 0.001$.

Pop	Location	Lat	Lon	N	A_r	H_O	H_E	F_{IS}	HL	sF_{IS}	sID	sPA	Sp	N_e	Census size
EZ	Egmond aan Zee	52.61	4.63	30	3.90	0.45	0.52	0.14***	0.48	0.25	0.09	0.19	0.037***	46	≥ 5000
EB	Egmond-Binnen	52.58	4.64	30	3.91	0.47	0.54	0.14***	0.48	0.25	0.14	-	0.040***	22	≥ 5000
GOLF	Kennemer Golf & Country Club	52.37	4.56	23	4.13	0.48	0.53	0.09*	0.47	0.17	0.06	-	0.013	32	≥ 100
VOG	Vogelenzang	52.34	4.57	30	4.43	0.44	0.56	0.22***	0.49	0.36	0.00	-	0.016*	330	≥ 5000
MVT	Noordwijk North	52.22	4.4	30	4.22	0.38	0.51	0.26***	0.54	0.41	0.32	-	0.015**	113	≥ 5000
NOO	Noordwijk South	52.22	4.42	30	3.36	0.40	0.44	0.10*	0.54	0.19	0.16	-	0.034**	31	≥ 5000
WAS	Wassenaar	52.14	4.35	30	3.28	0.33	0.41	0.19***	0.60	0.33	0.19	0.35	-0.005	105	≥ 5000
MEIJ	Meijendel	52.13	4.32	30	3.42	0.40	0.47	0.14***	0.55	0.25	0.14	-	0.038***	38	≥ 5000
MONP	Monster North	52.05	4.19	30	3.06	0.32	0.41	0.22***	0.65	0.36	0.34	-	0.037***	21	≥ 50
MON	Monster South	52.04	4.18	30	3.42	0.34	0.47	0.29***	0.60	0.45	0.15	-	0.033**	76	≥ 3000
OVO	Oostvoorne	51.91	4.07	30	2.85	0.37	0.41	0.11*	0.55	0.20	0.20	0.23	0.029**	15	≥ 500
BH	Burgh-Haamstede	51.69	3.69	30	2.60	0.30	0.40	0.24***	0.63	0.39	0.00	-	0.052***	10	≥ 1000
OKA	Oostkapelle	51.59	3.56	30	1.61	0.24	0.16	-0.46***	0.75	0.00	0.00	-	0.004	2	≥ 1000
PER	Dunes du Perroquet	51.08	2.53	30	2.09	0.14	0.29	0.53***	0.84	0.69	0.00	-	0.147***	2	≥ 500
CAL	Dunes du Calvaire	51.07	2.52	30	1.89	0.15	0.19	0.19**	0.83	0.32	0.41	-	0.028***	22	≥ 200
WULF	Dunes Dewulf	51.07	2.47	30	2.28	0.23	0.30	0.23***	0.72	0.38	0.30	0.61	0.022**	23	≥ 500
GRAV	Gravelines	51.02	2.13	30	1.00	0.00	0.00	-	1.00	-	-	-	-	1	30
ECAU	Dunes d'Ecault	50.66	1.57	30	1.30	0.10	0.09	-0.14	0.88	0.00	0.00	-	0.011	-	30
STEL	Stella-Plage	50.48	1.58	30	3.12	0.43	0.46	0.06	0.48	0.11	0.00	0.75	0.025**	19	≥ 300

Levels of genetic diversity, genetic differentiation and effective population size (*Ne*)

To identify rangewide spatial trends in population genetic structure, we calculated the following statistics using SPAGᴇDI version 1.5 (Hardy and Vekemans, 2002): allelic richness (A_r) per locus and population, observed heterozygosity (H_O), genetic diversity (H_E), intra-population fixation index (F_{IS}; Weir and Cockerham, 1984) and mean levels and pairwise population genetic differentiation (F_{ST}). Allelic richness was estimated using a rarefaction procedure based on a minimal sample size of 11 and 23 individuals for Rock samphire and Dune pansy, respectively. Significance of F_{IS} and F_{ST} estimates were assessed using 10 000 permutations of alleles within populations and of multilocus genotypes among populations, respectively. We chose to use F_{ST} since alternative measures of population differentiation tend to overestimate differentiation when mutation is high relative to migration rate, as is likely for microsatellite loci (Whitlock, 2011). To estimate whether individual level of inbreeding increased for marginal populations, we computed the homozygosity by locus (*HL,* Aparicio *et al.*, 2006), using the R package 'genhet' (Coulon, 2010). Likewise, to test whether contemporary effective population size (N_e) decreased towards the range edges, we estimated N_e based on levels of within-population linkage disequilibrium, as implemented in NᴇEsᴛɪᴍᴀᴛᴏʀ v2.1 (Do *et al.*, 2014), for populations with at least ten sampled individuals.

Population genetic affiliation

To identify broad-scale and cryptic geographical variation in allele frequencies depicting population boundaries, we performed a spatial principal component analysis (sPCA) as described in Jombart *et al.* (2008) and implemented in the R package 'adegenet' (Jombart, 2008). sPCA makes no assumptions with regard to linkage disequilibrium or departures from Hardy-Weinberg equilibrium. This analysis identifies independent synthetic components: those associated with the highest eigenvalues reflect positive spatial autocorrelation ("global structure") while those associated with the lowest eigenvalues depict repulsion patterns (Jombart *et al.*, 2008).

As a complementary approach, we tested whether the genetic differentiation among sampled locations mirrored the occurrence of distinct genetic pools by carrying out a non-spatially explicit Bayesian genetic clustering, as implemented in the software INSTRUCT (Gao *et al.*, 2007). In contrast to the seminal procedure of Pritchard *et al.* (2000), individual assignments to the most likely number *K* of clusters do not assume random mating and a

mean selfing rate can be estimated for each inferred cluster. We ran 35 Markov chain Monte Carlo (MCMC) chains for each value of *K*, ranging from 1 to the actual number of sampled populations for each species. Each run consisted in 200 000 initial burn-in iterations followed by 10^6 MCMC iterations. We used the *ad hoc* statistic *ΔK* (Evanno *et al.*, 2005) to assess the most likely number of clusters.

Large- and fine-scale spatial genetic structure

To assess the occurrence of within or among-population spatial genetic structure, we studied the relationship between genetic relatedness and geographical distance among individuals through spatial correlograms based on pairwise individual kinship coefficients (F_{ij}, Loiselle et al., 1995). Standard errors of F_{ij} estimations were assessed using a multilocus jackknife estimator and 95% confidence intervals were generated using 10 000 permutations of individual locations. To compare the strength of spatial genetic structure among populations, we calculated the *Sp* statistic which is independent of the sampling scheme, and described in Vekemans & Hardy (2004).

Assessment of recent migration rates among populations

To assess whether recent migration events among populations were asymmetrical from historical core populations to marginal populations, we used Bayesian inferences implemented in BᴀʏᴇsAss (Wilson and Rannala, 2003). This software estimates relative rates of gene flow over the last few generations, without requiring genetic equilibrium. We launched several runs of analysis including 20 million MCMC iterations with a burn-in of 4 million iterations and mixing parameters of 0.3 (0.6) for allele frequencies and 0.5 (0.7) for inbreeding coefficients in Dune pansy (respectively in Rock samphire).

Inference of mating system variation

To determine whether selfing rates increased towards the edges of geographic distribution ranges, we estimated within-population selfing rates (*s*) using three independent methods, one based on the within-population genotypic structure (sF_{IS}), the second being derived from the multilocus correlation structure (standardized identity disequilibrium, sID), the third relying on a progeny-array design (sPA). While sPA quantifies the amount of self-fertilized seeds, sF_{IS} and sID estimate the amount of selfing at later life stages that undergone natural selection thinning.

sF_{IS} was estimated from the classical relationship $s=2F_{IS}/(1+F_{IS})$ assuming inbreeding equilibrium in an infinite

population for which the mating system is thought to be the most salient source of inbreeding (Hedrick, 2011). sID was derived from maximum likelihood estimates based on the distribution of multilocus heterozygosity (identity disequilibrium; David *et al.*, 2007). sF_{IS} and sID estimates are thus based on a population structure approach. sPA was based on a progeny-array analysis using a set of maternal plants and offspring genotypes. Mating system parameters were estimated at the population level using a maximum-likelihood approach under a mixed-mating system model, using the MLTR v3.2 software (Ritland 2002).

sF_{IS} and sID were estimated for all populations, but sPA was only determined for five or six populations in each species (Tables 1 and 2). We chose to estimate sPA for a small number of large progeny arrays to better estimate individual selfing rates. 6 ± 1.58 sampled individuals per population were used as mother plants with 12.5 ± 2.1 seeds per plant, for a grand total of 506 and 375 genotyped seedlings for Rock samphire and Dune pansy, respectively. Finally, we also obtained an estimate of selfing rates at the level of the individual clusters inferred by INSTRUCT.
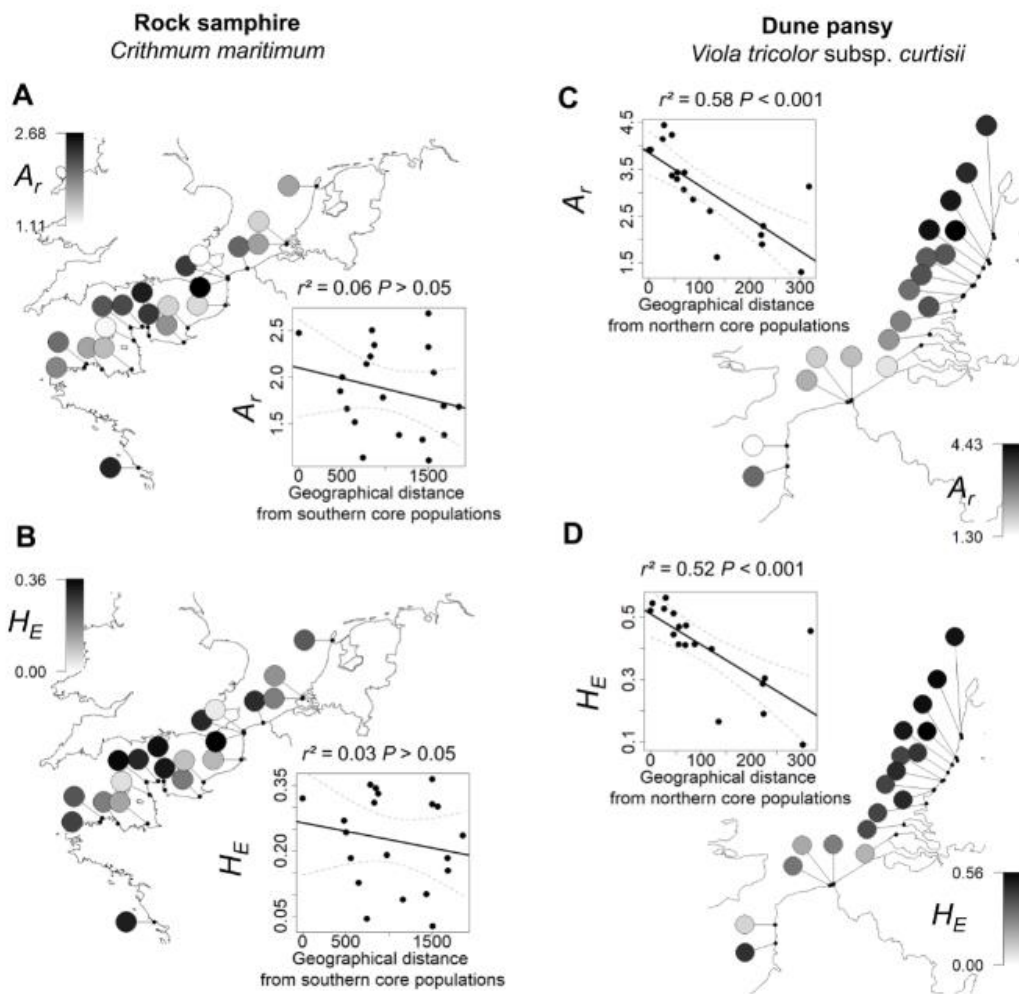
Figure 2: Geographical distribution of genetic diversity in populations of *Crithmum maritimum* (A-B) and *Viola tricolor* subsp. *curtisii* (C-D). A and C: allelic richness (A_r); B and D: expected heterozygosity (H_E). Insets show the estimates of genetic diversity with respect to the coastline geographical distance to central (core) populations; i.e. from the southernmost population for *Crithmum maritimum* and the northernmost population for *Viola tricolor* ssp. *curtisii*. For significant correlations, dashed lines indicate the 95% confidence interval.

RESULTS

Levels of genetic diversity, effective population size and genetic differentiation

In Rock samphire, moderate levels of genetic diversity were observed across loci (Table 1): mean allelic richness of 1.86 ± 0.47, mean H_e of 0.22 ± 0.11 and H_o of 0.13 ± 0.08. Linkage-based estimates of Ne were generally low (2 to 47, mean = 13.5, s.d. = 12.6). None of these estimates of genetic diversity significantly correlated with geographical location along the distribution range of this species (Figures 2A-B and S1B, D).

Dune pansy exhibited higher levels of genetic diversity (Table 2 and Figure 2C-D): mean allelic richness of 2.94 ± 1.01, mean H_e of 0.38 ± 0.16 and H_o of 0.31 ± 0.14. All of these estimates significantly decreased from central to marginal populations (Figures 2C-D and S2B; all at $P < 0.05$). All individuals from the trailing-edge population GRAV shared the same fully homozygous genotype. Yet, the most marginal population STEL had levels of genetic diversity similar to those found in central populations. Estimates of Ne varied greatly among populations (1-330, mean = 50; s.d. = 78), with no clear geographical trend (Figure S2D).

Populations were highly differentiated in both species: mean multilocus F_{ST} were 0.37 ± 0.20 in Rock samphire and 0.33 ± 0.20 in Dune pansy. In rock samphire, F_{ST} ranged from 0.03 to 0.90, and among 190 pairwise F_{ST} values, only two were not significant. The same held for Dune pansy: pairwise F_{ST} estimates ranged from 0.04 to 0.90 with only one non-significant pairwise F_{ST} after Bonferroni correction, indicating substantial genetic differentiation among almost all populations (Figures 4A, C). While pairwise F_{ST} values did not correlate with geographical distances in Rock samphire ($r_z = 0.024$, Mantel test, $P > 0.05$), they did in Dune pansy ($r_z = 0.500$, Mantel test, $P < 0.001$).
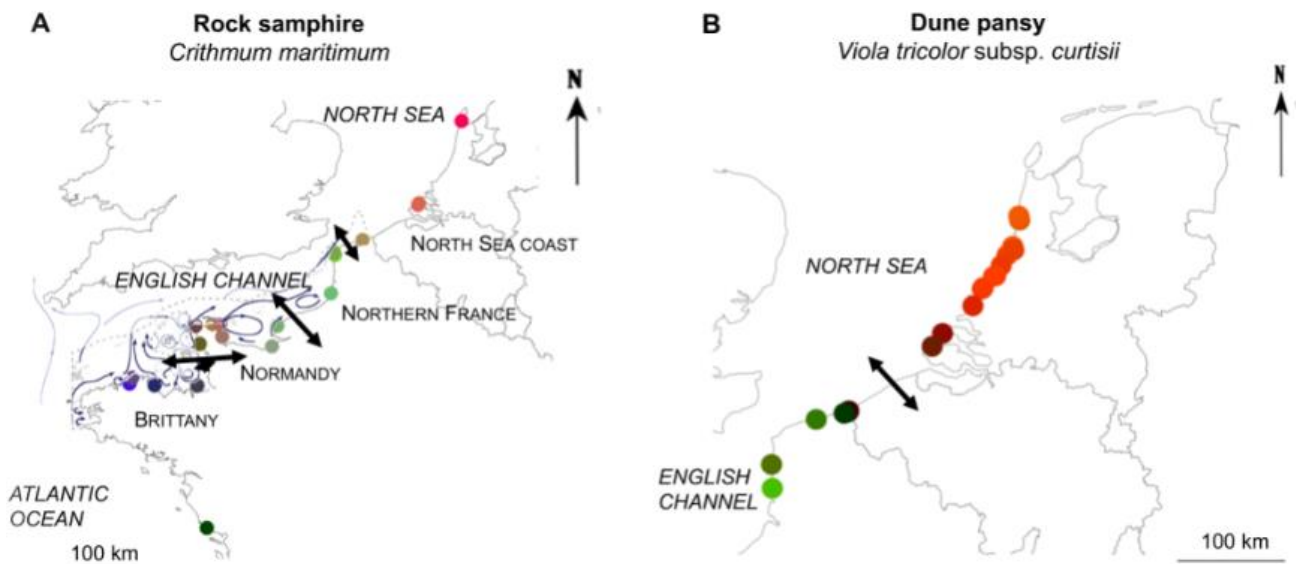
Figure 3: Population genetic affiliations using sPCA analysis for *Crithmum maritimum* (A) and for *Viola tricolor* subsp. *curtisii* (B). Population colors reflect their coordinates on the first three (*Crithmum maritimum*) or two (*Viola tricolor* subsp. *curtisii*) axes of the sPCA. Coordinates along these three (A) or two (B) axes were assigned to the Red, Green and Blue channels (only red and green were thus used in B). For *Crithmum maritimum,* the main sea surface currents are also shown (taken from Lazure & Desmare, 2012) as well as breaks between genetic clusters (black arrows).
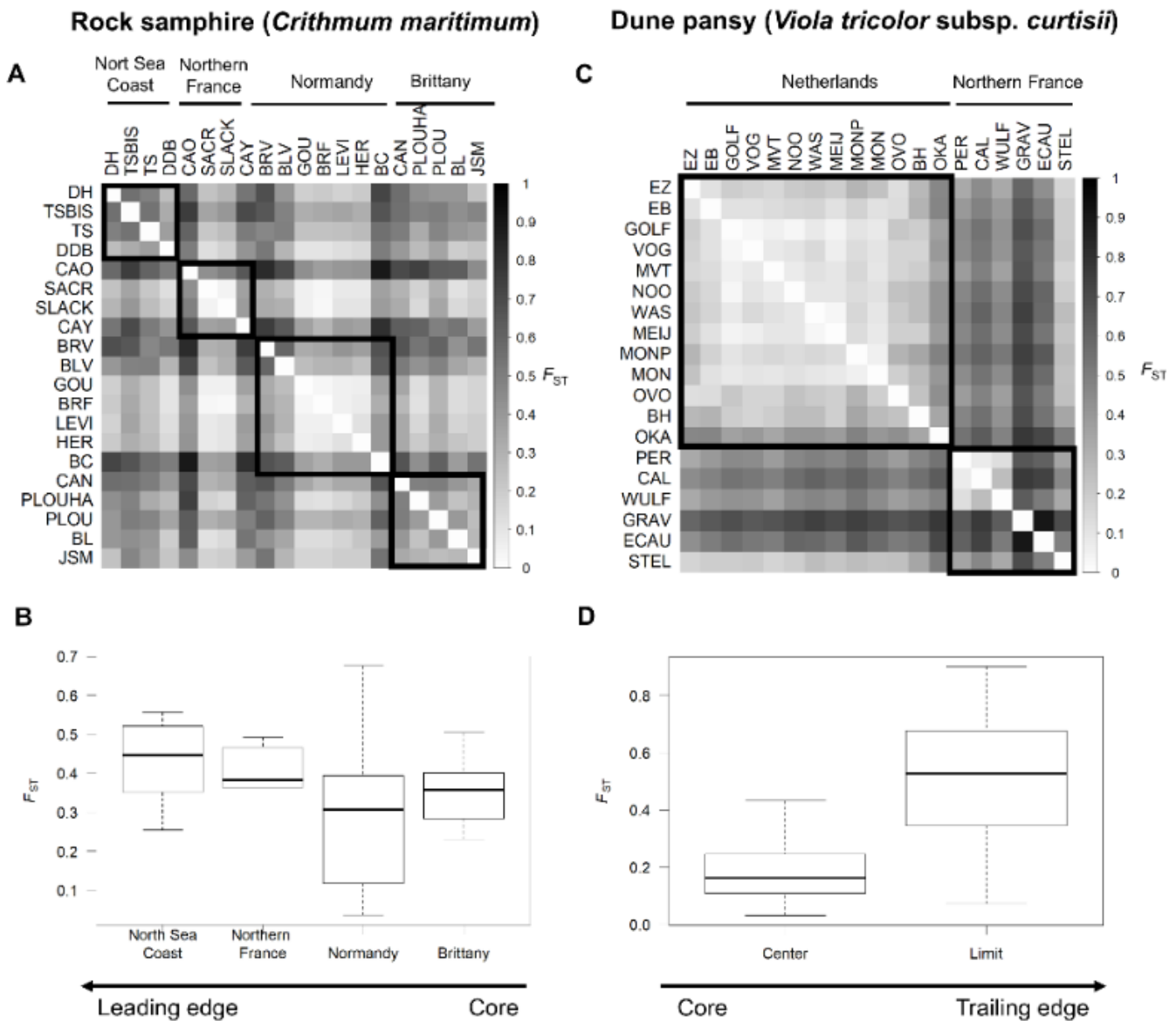
 Figure 4: Pairwise F_{ST} estimates for *Crithmum maritimum* (A-B) and *Viola tricolor* subsp. *curtisii* (C-D). A and C: Matrices of pairwise F_{ST} values for both species. Populations are listed from north to south in both cases. Black lines indicate population clusters, as determined by comparison of pairwise F_{ST} among neighboring populations. High F_{ST} values among two neighboring populations defined a break among clusters. Cluster names are given above the matrices. B and D: distribution of pairwise F_{ST} values within each cluster.

Population genetic affiliation and large- and fine-scale spatial genetic structure

Contrasting geographical partitions of populations were observed for the two focal species. Rock samphire showed a significant global structure (G-test = 0.11, $P = 0.024$) and four spatially structured groups were

identified by the first three axes of the sPCA (Moran's I = 0.72, 0.59, 0.49 with var = 0.29, 0.23 and 0.17 respectively; Figures 3A, S3): (i) southern populations from the Atlantic coast, (ii) neighboring populations from Normandy, (iii) scattered populations from northern France, (iv) isolated marginal Dutch populations. The same four groups were

obtained when analyzing pairwise F_{ST} values among neighboring populations (Figure 4A), with similar within-group mean pairwise F_{ST} (Figure 4B). Bayesian clustering accounting for partial selfing identified three main clusters that did not correspond to well-defined geographically delimited genetic entities, and that showed substantial selfing rates ranging from 0.65 to 0.78 (Figure S4).

Dune pansy showed striking geographical structuring with two differentiated lineages (Figure 3B) supported by the sPCA global test (G-test = 0.14, *P* < 0.001). The first two sPCA axes accounted for most of the spatial genetic patterning in the data (Moran's *I* = 0.88 and 0.69 with var = 0.77 and 0.18, respectively), with a genetic break between northern and southern populations occurring between populations MON and OVO, and a weak genetic discontinuity located more southerly, between populations WULF and GRAV (Figure S5). This suggested admixed ancestry for the southernmost Dutch populations and northernmost French populations. Bayesian clustering clearly confirmed these two clusters and consistently inferred mixed ancestry for all individuals of the southernmost Dutch population OKA (Figure S6). Selfing rate was of 0.34 and of 0.69 for the northern and southern

lineages, respectively. Besides, this analysis also suggested a mixed affiliation of the southernmost French population STEL, which accordingly showed low pairwise genetic differentiation with core Dutch populations (Figure 4C). Core Dutch populations were less differentiated than marginal populations (mean pairwise F_{ST} estimates of 0.20 and 0.54 respectively; *P* < 0.01; Figure 4D).

Both species displayed large-scale significant spatial genetic structure with a clear decrease in genetic similarity among individuals with increasing geographical distance (Figures 5A, 5C). Positive spatial autocorrelation only occurred at the intra-population level in Rock samphire (Figure 5A). When performing this analysis at the level of genetic clusters identified above, a stronger signal of isolation by distance was observed for both species (Figures 5B, 5D). Spatial genetic structure was clearly stronger for trailing-edge populations than for core populations in Dune pansy (Figure 5D). Within populations, both species showed a significant pattern of isolation by distance in 63% of populations of Rock samphire and in 78% of Dune pansy populations, as indicated by the *Sp* statistic. *Sp* did not show any geographical trend for either species (Tables 1 and 2).
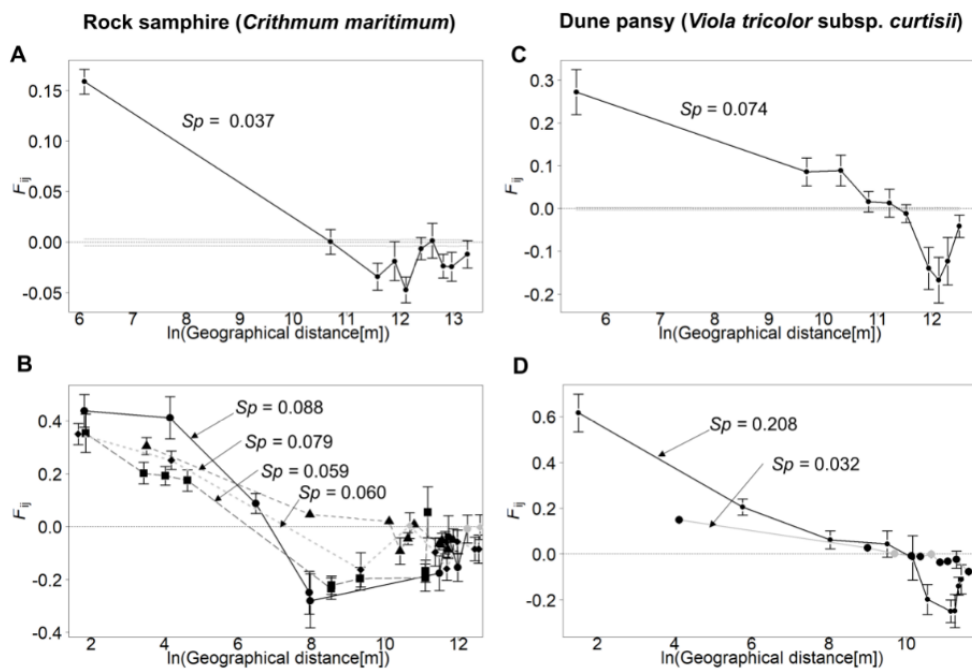

Figure 5: Spatial autocorrelograms depicting the relationship between pairwise kinship coefficients F_{ij} (Loiselle *et al.*, 1995) among individuals of Rock samphire (A-B) or Dune pansy (C-D), and the logarithm of coastal geographical distances. A and C: among all individual samples; B and D: within spatial clusters determined by the sPCA analysis. Solid lines correspond to the most marginal cluster, and dashed and dotted lines to the more central clusters. On all autocorrelograms, black symbols indicate values of F_{ij} that are significantly different from zero. The *Sp* statistic is given for each autocorrelogram (all at *P* < 0.05).

Recent migration rates

Estimated migration rates among populations were generally low: the proportion of non-migrants ranged from 67 to 88% in both species (Tables S2 and S3). For Dune pansy, a mean of 19% immigration events was observed, with the central populations WAS, MEIJ and MONP contributing to emigration to diverse central populations (Table S2). The trailing-edge population CAL was inferred to send migrants to close neighboring populations. Surprisingly, populations OKA and STEL, which appeared of mixed ancestry, were not inferred to send nor to receive large proportions of migrants. For Rock samphire, inferred migration rates were slightly larger, with a mean incoming gene flow of 22% and strong evidence for asymmetrical gene flow coming from Normandy (Table S3). Indeed, populations from the Normandy peninsula (HER, LEVI, BRF, GOU and BRV) sent migrants to most other populations, with dispersal events occurring randomly, irrespective of population location. The smallest expanding range-edge populations did not show higher immigration rates than core populations (20 to 23% immigrants in the four population clusters identified by the sPCA; Table S3).

Geographical variation in mating system along the distribution range

In Rock samphire, significant departures from Hardy-Weinberg (HW) equilibrium were detected in all but one population, with substantial F_{IS} estimates ranging from 0.14 to 0.88 (0.41 ± 0.22, all at $P < 0.05$; Table 1 & Figure S1A). The only population that did not show significant departures from HW expectations was PLOUHA ($F_{IS} = 0.17$), probably due to sampling effects: only 11 individuals were sampled out of a much larger population of inaccessible plants on a cliff. Individual internal relatedness estimates (*IR*) were high, ranging from 0.34 to 0.96 (0.64 ± 0.21; Table 1), but did not show any spatial trends (Figure S1C). Selfing rate estimates supported a predominant self-fertilization mating system, regardless of the statistical method used to infer them. Mean selfing rate over populations was 0.57 ± 0.20, 0.53 ± 0.26 and 0.84 ± 0.10 using sF_{IS}, sID and sPA metrics, respectively (Figure 6A and Table 1). Selfing rates based on F_{IS} and on identity disequilibrium were strongly correlated ($r^2 = 0.78$, $P < 0.001$; Figure S7A). However, selfing rates estimated from progeny array analyses did not correlate with and were generally much higher than the former two estimates (Figures 6 and S7A). Although selfing rates based on F_{IS} and on identity disequilibrium did not show any significant geographical trends, selfing rates derived from progeny arrays indicated a marginal trend for increasing selfing rates in leading-edge populations ($r^2 = 0.54$, $P = 0.097$; Figure S7B).
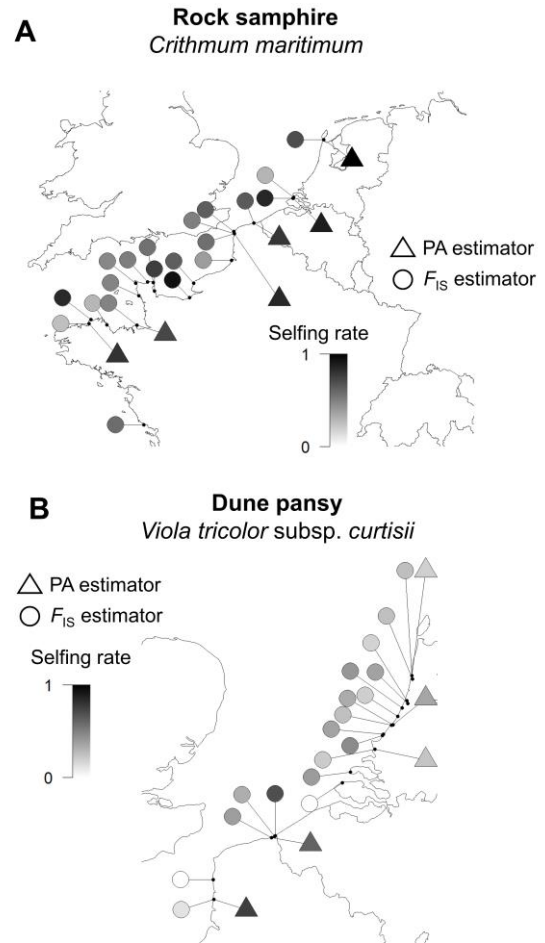
Figure 6: Geographical distribution of selfing rates estimated using the intra-population fixation index F_{IS} (circles) and progeny array analyses (triangles) in *Crithmum maritimum* (A) and in *Viola tricolor* subsp. *curtisii* (B).

Dune pansy showed a genotypic structure suggestive of a more mixed-mating system with a lower propensity for selfing. Significant departures from HW expectations were observed in 17 out of 19 populations, with F_{IS} values ranging from 0.09 to 0.53 (0.20 ± 0.11) but no geographical trend emerged (Table 2 & Figure S2A). One population (OKA) that was previously identified as being strongly admixed was characterized by a significant heterozygote excess, with a mean multilocus F_{IS} value of -0.46 ($P < 0.001$). Overall, these results are consistent with relatively high individual *IR* estimates, varying from 0.19 to 1.00 (0.45 ± 0.22; Table 2) and significantly increasing from central to trailing-edge populations ($r^2 = 0.50$, $P < 0.001$; Figure S2C). Selfing rates estimated by F_{IS} and identity disequilibrium methods were moderately correlated ($r^2 = 0.23$, $P = 0.06$; Figure S8A) and indicated a mixed-mating system (mean s$F_{IS} = 0.27 ± 0.17$, sID = 0.14 ± 0.13),

but did not show any significant geographical patterning from core to edge populations (Figures 6B and S8B). Nonetheless, the progeny-based selfing rate estimations (mean sPA = 0.42 ± 0.25) showed a significant increase in selfing rates towards the receding range margin ($P < 0.01$; Figures 6B and S8B).

DISCUSSION
Variation of genetic diversity and effective population size along the geographical range

Due to geographical isolation and reduced census population size, lower levels of genetic diversity and effective population size, and higher levels of genetic differentiation are expected within and among static marginal populations relative to historical core populations (Le Corre and Kremer, 1998; Pannell and Charlesworth, 2000; Eckert *et al.*, 2008). These expected patterns of genetic structure have been well established for invasive species or species that underwent historical range shifts due to post-glacial range expansion (e.g. Hewitt, 2000; Jump *et al.*, 2003; Griffin and Willi, 2014; Samis *et al.*, 2016; López-Villalobos and Eckert, 2018). However, empirical investigations of genetic structure of dynamic native species' range over contemporary time-scales are still lacking, especially for trailing edges of currently receding species (Hampe and Petit, 2005; Arenas *et al.*, 2012; Vilà-Cabrera *et al.*, 2019).

Interestingly, no evidence of spatial trends in genetic diversity or N_e was observed across the range-wide distribution of Rock samphire. N_e estimates were particularly low, a finding expected for perennial species with a large propensity for selfing (Hamrick and Godt, 1996; Griffin and Willi, 2014; Ellegren and Galtier, 2016). The lack of spatial trends in genetic diversity may be attributable to efficient seed dispersal by hydrochory (Kudoh and Whigham, 1997; Favre-Bac *et al.*, 2016). Occasional long-distance dispersal events mediated by seeds drifting along major sea currents can partially offset the effects of geographical isolation of marginal populations (Fievet *et al.*, 2007; Leys *et al.*, 2014). In line with these confounding effects, no significant pattern of isolation by distance was observed among Rock samphire populations, and a significant spatial genetic structure only occurred at the intra-population level. Finally, the lack of reduced N_e at leading range margins suggested that newly established populations are likely to be founded by several individuals. The mode of colonization has theoretically been recognized as a major factor influencing the level of genetic diversity and the amount of population differentiation, especially at range margin (Pannell and Charlesworth, 2000). Long-distance seed dispersal by hydrochory may thus compensate for spatially restricted pollen flow and lead to departures from the common view of reduced genetic diversity that applies for historical leading-edge populations. This is predicted under a migrant-pool model where colonists are drawn from a random sample of the whole metapopulation (Whitlock and McCauley, 1990). Empirical support for a migrant-pool model was observed for historical cytoplasmic variation in sea beet, a coastal plant species with similar life-history traits (Leys *et al.*, 2014). Our study demonstrates that efficient long-distance dispersal abilities may attenuate contemporary changes in genetic structure expected at expanding leading edges owing to genetic drift (see also Bialozyt *et al.*, 2006 for theoretical expectations).

In contrast, under a relaxed propagule-pool model where new populations are founded from few sources, genetic differentiation is always expected to increase relative to an island model (Slatkin, 1977; Whitlock and McCauley, 1990). Dune pansy seeds are dispersed over very short spatial distances, first by fruit explosion then by myrmecochory (Oostermeijer, 1989; Rix, 2014). Consistently, Dune pansy showed a strong pattern of isolation by distance. This suggests spatially restricted dispersal enhancing genetic drift effects, in line with patterns of genetic structure observed in various plant species with similar life-history traits (Hamrick and Godt, 1996; Lönn and Prentice, 2002; Hirai *et al.*, 2012; Auffret *et al.*, 2017). As observed for historical trailing edges (e.g. Griffin and Willi, 2014), a significant decrease in genetic diversity was observed towards the trailing edge of the Dune pansy. One population in particular exemplified this pattern, because all sampled individuals shared the same fully homozygous genotype (population GRAV). However, the southernmost Dune pansy population (STEL), still exhibited levels of genetic diversity comparable to core populations. This population may benefit from being situated in an unusually large unmanaged dune complex, and may have retained its former rear-edge polymorphism (see Hampe and Petit, 2005; Vilà-Cabrera *et al.*, 2019). However, we did not observe any private alleles in this population, as would be expected for static remnant marginal populations (Hampe and Petit, 2005). Beyond this legacy of past genetic diversity and of past population connectedness, another non-exclusive hypothesis may involve genetic admixture, *e.g.* through human-mediated sand transport. Overall and beyond a snapshot of neutral genetic variation, understanding adaptive differentiation will help design efficient management strategies to decide which dune pansy populations should be used as seed sources for translocation, supplementation or assisted migration to preserve currently receding trailing-edge populations (Vilà-Cabrera *et al.*, 2019).

Large- and fine-scale spatial genetic structure

Pollen and seed dispersal distance are crucial in determining population genetic connectedness in light of ongoing rapid environmental changes and alteration (Vekemans and Hardy, 2004; Favre-Bac *et al.*, 2016; Auffret *et al.*, 2017). Myrmecochores are typically poor dispersers and ant-mediated seed dispersal does not facilitate range expansion (Warren *et al.*, 2010). In a retracting and shortly-dispersed species such as Dune pansy, striking biogeographical patterns are thus expected (Hamrick and Godt, 1996; Hewitt, 2000; Vekemans and Hardy, 2004). The recent migration rates among populations indeed indicated low levels of contemporary gene flow restricted to the nearest neighboring populations through a classical stepping-stone model. Moreover, a genetic discontinuity separated core Dutch populations from marginal French populations, with admixed ancestry for an intermediate population located in between. Finally, pairwise F_{ST} estimates suggested stronger level of genetic differentiation among trailing-edge populations than among core populations, consistent with theoretical and empirical expectations of increasing spatial isolation of marginal receding populations, especially when range contraction is slow (Arenas *et al.*, 2012; Samis *et al.*, 2016). In contrast, gene flow was not impeded among central populations benefiting from nearly continuous suitable dune habitats, with migration events occurring over long distances. Consistent with increasing geographical isolation, spatial genetic structure increased towards southern marginal populations. Altogether, patterns of contemporary genetic structure for this species perfectly mirrored what is expected for historical range contraction (Hampe and Petit, 2005; Griffin and Willi, 2014).

A somewhat different pattern of large-scale spatial genetic structure was observed in Rock samphire. Rock samphire is an entomophilous species with spatially-restricted pollen flow mostly occurring within populations. As such, a significant spatial genetic structure due to kinship structure was observed within most populations. However, no clear biogeographical patterns related to either recent range expansion or postglacial recolonization were identified using non-spatially explicit Bayesian clustering. Our results thus contrasted to most studies classically based on the 'abundant center' hypothesis or on spreading invasive species (Jump *et al.*, 2003; Eckert *et al.*, 2008; Griffin and Willi, 2014; Samis *et al.*, 2016). This lack of global structure is consistent with theoretical expectations under a migrant-pool model and with relatively high estimated levels of contemporary rangewide migration events (Whitlock and McCauley, 1990; Moeller *et al.*, 2011). However, sPCA analyses with spatial priors allowed us to depict broad genetic breaks, matching main marine currents trajectories along the Atlantic, English channel and North sea coastlines, as observed in hydrochorous coastal plant species with similar habitat requirements (Ridley, 1930; Kadereit *et al.*, 2005; Leys *et al.*, 2014). A first break separated southern populations from Brittany and Normandy, consistent with long-term sea-surface current forking. Populations from Normandy appeared more genetically related with moderate pairwise genetic differentiation, which may suggest efficient connectivity through swirling currents (Salomon and Breton, 1993; Fievet *et al.*, 2007). Altogether, our results suggest that contemporary long-distance seed drifting, together with high seed longevity, partly erased the patterns of genetic variation expected under a simple isolation by distance model under drift/gene flow equilibrium for historical range shifts (Le Corre and Kremer, 1998; Bialozyt *et al.*, 2006; Moeller *et al.*, 2011).

Mating system across the geographical range

Geographical variation in mating system may result from a diverse array of selective pressures, and determine opportunities for further adaptive evolution in rapidly changing human-altered environments (Jain, 1976; Eckert *et al.*, 2010; Grossenbacher *et al.*, 2015; Pannell, 2015; Moeller *et al.*, 2017). Both Rock samphire and Dune pansy showed mixed-mating systems, as demonstrated by high mean F_{IS} values and homozygosity by locus. Accordingly, both direct (progeny-array based) and indirect (population-structure based) estimates of selfing rate point to substantial selfing, especially in Rock samphire. In contrast to what is observed in mixed-mating species such as Dune pansy, predominant selfing increases the among-population genetic variance, enhances local inbreeding level, and decreases pollen flow. Therefore, Rock samphire populations were strongly genetically structured (mean $F_{ST} = 0.37$), harbored significant intra-population kinship structure and did not follow a large-scale isolation by distance pattern reflecting a gene flow/drift equilibrium. Along with reduced N_e, such findings are typical of predominantly selfing perennial species (Jain, 1976; Hamrick and Godt, 1996; Vekemans and Hardy, 2004; Griffin and Willi, 2014; Ellegren and Galtier, 2016).

In Rock samphire, selfing rates estimated from population genetic structure all exceeded 25% and reached up to 94%. In a colonizing species, low mate availability and pollen limitation may favor selfers in expanding leading-edge populations (Eckert *et al.*, 2008; Pannell, 2015; Moeller *et al.*, 2017). Nonetheless, indirect estimates of selfing rates did not increase towards leading-edge populations, as expected for newly established invasive species or historical expansion front following the ice retreat after the last glacial maximum (e.g. Griffin and Willi, 2014; see however Colautti *et al.*, 2010). Our results thus

suggested attenuated founder effects during ongoing colonization. Indeed, the possibility of long-distance seed dispersal through marine hydrochory makes this species a potentially efficient colonizer (Ridley, 1930; Kadereit *et al.*, 2005). Multiple colonization events from diverse sources may offset drift effects and mate limitation, as theoretically expected under a migrant-pool model (Baker, 1955; Whitlock and McCauley, 1990; Bialozyt *et al.*, 2006; Pannell, 2015). Thus, contemporary expanding species may not always follow the expected pattern of increased selfing in stable leading-edge populations, either because (i) some traits related to dispersal make them efficient colonizers with large populations near the leading range limits (e.g. Herlihy and Eckert, 2005), (ii) population expansion is not limited by the availability of pollinators and compatible mates (Colautti *et al.*, 2010; Moeller *et al.*, 2012), or (iii) colonization events are old enough for plants to have shifted back towards a more open mating system (Hargreaves and Eckert, 2014; Pannell, 2015). For the above reasons, Rock samphire populations did not show the expected pattern of increased selfing rates towards the leading edge of the species' distribution.

Owing to urbanization and to diverse dune management strategies along the coast of Northern France, trailing-edge Dune pansy populations are more geographically isolated and generally smaller than core populations. In this mixed-mating species, mate limitation is expected in trailing-edge populations facing anthropogenic disturbances, which would drive an evolutionary shift towards more selfed progeny, as observed in other species, including coastal Dune plants (Darling *et al.*, 2008; Eckert *et al.*, 2010; Griffin and Willi, 2014; López-Villalobos and Eckert, 2018). Direct estimates based on progeny arrays indeed showed increased selfing rates towards currently receding trailing-edge populations, indicating pollen limitation and seed discounting in harsh marginal environments and suggesting small N_e, as often observed for historical rear edges (Hampe and Petit, 2005; Gaston, 2009; Griffin and Willi, 2014). However, caution has to be taken: indirect estimates of selfing rates based on population genetic structure did not show this expected increase in selfing rates in contemporary receding trailing-edge populations of Dune pansy. This highlights the need to use both direct and indirect estimators of selfing rates to avoid over-interpretation (Bürkli *et al.*, 2017).

Selfing rate estimates using progeny arrays were also consistently higher than those estimated using population structure. Beyond departures from a pure inbreeding equilibrium (Hedrick, 2011), this may be due to the time-lag necessary to approach genetic equilibrium in receding or expanding populations (Pannell, 2015).

Alternatively, this may suggest the existence of some level of inbreeding depression acting at early developmental stages in both species, with selfed offspring showing lower survival than outcrossed offspring. Thus, thinning effects may explain why the difference in estimated selfing rates between central and marginal populations diminishes along life stages. In line with the conclusions of Bürkli *et al.* (2017), our results suggest that direct and indirect selfing rate estimates are not necessarily correlated, because they capture selfing rates at different life stages. To draw correct inferences on mating system, selfing rates need to be estimated at different life stages using both direct and indirect approaches, especially for populations with contemporary dynamic geographical ranges.

Conclusion

Patterns of genetic structure and mating system are rarely studied for native species undergoing retracting or expanding range dynamics at contemporary time-scales. A reduction in genetic diversity and an increase in genetic differentiation in marginal populations, expected under the 'abundant center' paradigm, was only observed near the trailing edge of the receding Dune pansy. Dune pansy and Rock samphire did not show the expected increase in selfing rates in marginal populations when considering estimates based on population genetic structure. However, progeny arrays suggested that most seeds were sired by selfing in currently shifting marginal populations, which may indicate the occurrence of some degree of inbreeding depression.

Altogether, this study lends support to the importance of life-history traits related to dispersal abilities in shaping contemporary genetic structure in a changing world. Lower genetic diversity, higher selfing rate and higher genetic differentiation can reasonably be expected in marginal populations of fragmented and short-dispersed taxa. Nonetheless, these assumptions do not necessarily hold for self-compatible species with efficient dispersal capabilities, such as Rock samphire (reviewed in Grossenbacher *et al.*, 2015; Moeller *et al.*, 2017).

REFERENCES

Aparicio JM, Ortego J, Cordero PJ (2006). What should we weigh to estimate heterozygosity, alleles or loci? *Mol Ecol* **15**: 4659–4665.

Arenas M, Ray N, Currat M, Excoffier L (2012). Consequences of range contractions and range shifts on molecular diversity. *Mol Biol Evol* **29**: 207–218.

Auffret AG, Rico Y, Bullock JM, Hooftman DAP, Pakeman RJ, Soons MB, *et al.* (2017). Plant functional connectivity – integrating landscape structure and effective dispersal. *J Ecol* **105**: 1648–1656.

Baker HG (1955). Self-compatibility and establishment after 'long-distance' dispersal. *Evolution (N Y)* **9**: 347–349.

Bialozyt R, Ziegenhagen B, Petit RJ (2006). Contrasting effects of long distance seed dispersal on genetic diversity during range expansion. *J Evol Biol* **19**: 12–20.

Brown JH (1984). On the relationship between abundance and distribution of species. *Am Nat* **124**: 255.

Bürkli A, Sieber N, Seppälä K, Jokela J (2017). Comparing direct and indirect selfing rate estimates: when are population-structure estimates reliable? *Heredity (Edinb)* **118**: 525–533.

Cheptou P-O, Massol F (2009). Pollination fluctuations drive evolutionary syndromes linking dispersal and mating system. *Am Nat* **174**: 46–55.

Colautti RI, White NA, Barrett SCH (2010). Variation of self-incompatibility within invasive populations of purple loosestrife (*Lythrum salicaria* L.) from Eastern North America. *Int J Plant Sci* **171**: 158–166.

Le Corre V, Kremer A (1998). Cumulative effects of founding events during colonisation on genetic diversity and differentiation in an island and stepping-stone model. *J Evol Biol* **11**: 495–512.

Coulon A (2010). GENHET: An easy-to-use R function to estimate individual heterozygosity. *Mol Ecol Resour* **10**: 167–169.

Darling E, Samis KE, Eckert CG (2008). Increased seed dispersal potential towards geographic range limits in a Pacific coast dune plant. *New Phytol* **178**: 424–435.

David P, Pujol B, Viard F, Castella V, Goudet J (2007). Reliable selfing rate estimates from imperfect population genetic data. *Mol Ecol* **16**: 2474–2487.

Do C, Waples RS, Peel D, Macbeth GM, Tillett BJ, Ovenden JR (2014). NeEstimator v2: Re-implementation of software for the estimation of contemporary effective population size (*Ne*) from genetic data. *Mol Ecol Resour* **14**: 209–214.

Eckert CG, Kalisz S, Geber MA, Sargent R, Elle E, Cheptou PO, *et al.* (2010). Plant mating systems in a changing world. *Trends Ecol Evol* **25**: 35–43.

Eckert CG, Samis KE, Lougheed SC (2008). Genetic variation across species' geographical ranges: the central-marginal hypothesis and beyond. *Mol Ecol* **17**: 1170–1188.

Ellegren H, Galtier N (2016). Determinants of genetic diversity. *Nat Rev Genet* **17**: 422–433.

Evanno G, Regnaut S, Goudet J (2005). Detecting the number of clusters of individuals using the software STRUCTURE: a simulation study. *Mol Ecol* **14**: 2611–2620.

Favre-Bac L, Mony C, Ernoult A, Burel F, Arnaud J-F (2016). Ditch network sustains functional connectivity and influences patterns of gene flow in an intensive agricultural landscape. *Heredity (Edinb)* **116**: 200–212.

Fievet V, Touzet P, Arnaud JF, Cuguen J (2007). Spatial analysis of nuclear and cytoplasmic DNA diversity in wild sea beet (*Beta vulgaris* ssp. *maritima*) populations: Do marine currents shape the genetic structure? *Mol Ecol* **16**: 1847–1864.

Gao H, Williamson S, Bustamante CD (2007). A Markov Chain Monte Carlo approach for joint inference of population structure and inbreeding rates from multilocus genotype data. *Genetics* **176**: 1635–1651.

Gaston KJ (2009). Geographic range limits: achieving synthesis. *Proc R Soc B Biol Sci* **276**: 1395–1406.

Griffin PC, Willi Y (2014). Evolutionary shifts to self-fertilisation restricted to geographic range margins in North American *Arabidopsis lyrata*. *Ecol Lett* **17**: 484–490.

Grossenbacher D, Runquist RB, Goldberg EE, Brandvain Y (2015). Geographic range size is predicted by plant mating system. *Ecol Lett* **18**: 706–713.

Hampe A, Petit RJ (2005). Conserving biodiversity under climate change: the rear edge matters. *Ecol Lett* **8**: 461–467.

Hamrick J, Godt MJW (1996). Effects of life history traits on genetic diversity in plant species. *Philos Trans R Soc B* **351**: 1291–1298.

Hardy OJ, Vekemans X (2002). Spagedi: a versatile computer program to analyse spatial genetic structure at the individual or population levels. *Mol Ecol Notes* **2**: 618–620.

Hargreaves AL, Eckert CG (2014). Evolution of dispersal and mating systems along geographic gradients: implications for shifting ranges. *Funct Ecol* **28**: 5–21.

Hedrick PW (2011). *Genetics of Populations, 4th edition*, 4th Editio. Jones & Bartlett Publishers, Inc.: Sudbury, MA.

Herlihy C, Eckert C (2005). Evolution of self-fertilization at geographical range margins? A comparison of demographic, floral, and mating system variables in central vs. peripheral populations of *Aquilegia canadensis* (Ranunculaceae). *Am J Bot* **92**: 744–751.

Hewitt G (2000). The genetic legacy of the Quaternary ice ages. *Nature* **405**: 907–913.

Hirai M, Kubo N, Ohsako T, Utsumi T (2012). Genetic diversity of the endangered coastal violet *Viola grayi* Franchet et Savatier (Violaceae) and its genetic relationship to the species in subsection Rostratae. *Conserv Genet* **13**: 837–848.

Hopper J V., McCue KF, Pratt PD, Duchesne P, Grosholz ED, Hufbauer RA (2019). Into the weeds: Matching importation history to genetic consequences and pathways in two widely used biological control agents. *Evol Appl* **12**: 773–790.

Jain SK (1976). The evolution of inbreeding in plants. *Annu Rev Ecol Syst* **7**: 469–495.

Jombart T (2008). Adegenet: a R package for the multivariate analysis of genetic markers. *Bioinformatics* **24**: 1403–1405.

Jombart T, Devillard S, Dufour AB, Pontier D (2008). Revealing cryptic spatial patterns in genetic variability by a new multivariate method. *Heredity (Edinb)* **101**: 92–103.

Jump AS, Peñuelas J (2005). Running to stand still: adaptation and the response of plants to rapid climate change. *Ecol Lett* **8**: 1010–1020.

Jump AS, Woodward FI, Burke T (2003). *Cirsium* species show disparity in patterns of genetic variation at their range-edge, despite similar patterns of reproduction and isolation. *New Phytol* **160**: 359–370.

Kadereit JW, Arafeh R, Somogyi G, Westberg E, Westberg E, Kadereit JW (2005). Terrestrial growth and marine dispersal? Comparative phylogeography of five coastal plant species at a European scale. *Taxon* **54**: 861–876.

Kawecki TJ (2008). Adaptation to marginal habitats. *Annu Rev Ecol Evol Syst* **39**: 321–342.

Kudoh H, Whigham DF (1997). Microgeographic genetic structure and gene flow in *Hibiscus moscheutos* (Malvaceae) populations. *Am J Bot* **84**: 1285–1293.

Lambinon J, Verloove F (2012). *Nouvelle flore de la Belgique, du G.-D. de Luxembourg, du nord de la France et des régions voisines*, 6th edn. Jardin Botanique National de Belgique: Meise, Belgium.

Latron M, Arnaud J-F, Ferla H, Godé C, Duputié A (2018). Polymorphic nuclear markers for coastal plant species with dynamic geographic distributions, the rock samphire (*Crithmum maritimum*) and the vulnerable dune pansy (*Viola tricolor* subsp. *curtisii*). *Mol Biol Rep* **45**: 203–209.

Lazure P, Desmare S (2012). Caractéristiques physiques et état écologique - Manche - Mer du Nord - Etat physique et chimique, caractéristiques physiques, courantologie. Ifremer/Agence des aires marines protégées.

Levin DA (2012). Mating system shifts on the trailing edge. *Ann Bot* **109**: 613–620.

Leys M, Petit EJ, El-Bahloul Y, Liso C, Fournet S, Arnaud JF (2014). Spatial genetic structure in *Beta vulgaris* subsp. *maritima* and *Beta macrocarpa* reveals the effect of contrasting mating system, influence of marine currents, and footprints of postglacial recolonization routes. *Ecol Evol* **4**: 1828–1852.

Loiselle BA, Sork VL, John N, Graham C (1995). Spatial genetic structure of a tropical understory shrub, *Psychotria officinalis* (Rubiaceae). *Am J Bot* **82**: 1420–1425.

Lönn M, Prentice HC (2002). Gene diversity and demographic turnover in central and peripheral populations of the perennial herb *Gypsophila fastigiata*. *Oikos* **99**: 489–498.

López-Villalobos A, Eckert CG (2018). Consequences of multiple mating-system shifts for population and range-wide genetic structure in a coastal dune plant. *Mol Ecol* **27**: 675–693.

Moeller DA, Briscoe Runquist RD, Moe AM, Geber MA, Goodwillie C, Cheptou PO, *et al.* (2017). Global biogeography of mating system variation in seed plants. *Ecol Lett* **20**: 375–384.

Moeller DA, Geber MA, Eckhart VM, Tiffin P (2012). Reduced pollinator service and elevated pollen limitation at the geographic range limit of an annual plant. *Ecology* **93**: 1036–1048.

Moeller DA, Geber MA, Tiffin P (2011). Population genetics and the evolution of geographic range limits in an annual plant. *Am Nat* **178**: S44–S57.

Oostermeijer JGB (1989). Myrmecochory in *Polygala vulgaris* L., *Luzula campestris* (L.) DC. and *Viola curtisii* Forster in a Dutch dune area. *Oecologia* **78**: 302–311.

Pannell JR (2015). Evolution of the mating system in colonizing plants. *Mol Ecol* **24**: 2018–2037.

Pannell JR, Barrett SCH (1998). Baker's law revisited: reproductive assurance in a metapopulation. *Evolution (N Y)* **52**: 657–668.

Pannell JR, Charlesworth B (2000). Effects of metapopulation processes on measures of genetic diversity. *Philos Trans R Soc B Biol Sci* **355**: 1851–1864.

Park DS, Ellison AM, Davis CC (2018). Mating system does not predict niche breath. *Glob Ecol Biogeogr* **27**: 804–813.

Phillips BL, Brown GP, Shine R (2010). Life-history evolution in range-shifting populations. *Ecology* **91**: 1617–1627.

Pritchard JK, Stephens M, Donnelly P (2000). Inference of population structure using multilocus genotype data. *Genetics* **155**: 945–959.

Ridley (1930). *The dispersal of plants throughout the world*. L. Reeve & Company, Limited: Ashford, Kent.

Rix M (2014). *Viola tricolor* subsp. *curtisii* (Violaceae). *Curtis's Bot Mag* **31**: 17–25.

Rodger JG, Landi P, Hui C (2018). Heterogeneity in local density allows a positive evolutionary relationship between self-fertilisation and dispersal. *Evolution (N Y)* **72**: 1784–1800.

Sagarin RD, Gaines SD, Gaylord B (2006). Moving beyond assumptions to understand abundance distributions across the ranges of species. *Trends Ecol Evol* **21**: 524–530.

Salomon JC, Breton M (1993). An atlas of long-term currents in the Channel. *Oceanol Acta* **16**: 439–448.

Samis KE, López-Villalobos A, Eckert CG (2016). Strong genetic differentiation but not local adaptation toward the range limit of a coastal dune plant. *Evolution (N Y)* **70**: 2520–2536.

Slatkin M (1977). Gene flow and genetic drift in a species subject to frequent local extinctions. *Theor Popul Biol* **12**: 253–262.

Steinbauer MJ, Grytnes JA, Jurasinski G, Kulonen A, Lenoir J, Pauli H, *et al.* (2018). Accelerated increase in plant species richness on mountain summits is linked to warming. *Nature* **556**: 231–234.

Vekemans X, Hardy OJ (2004). New insights from fine-scale spatial genetic structure analyses in plant populations. *Mol Ecol* **13**: 921–935.

Vilà-Cabrera A, Premoli AC, Jump AS (2019). Refining predictions of population decline at species' rear edges. *Glob Chang Biol* **in press**.

Warren RJ, Giladi I, Bradford MA (2010). Ant-mediated seed dispersal does not facilitate niche expansion. *J Ecol* **98**: 1178–1185.

Weir BS, Cockerham CC (1984). Estimating *F*-statistics for the analysis of population structure. *Evolution (N Y)* **38**: 1358–1370.

Whitlock MC (2011). G′$_{ST}$ and D do not replace FST. *Mol Ecol* **20**: 1083–1091.

Whitlock MC, McCauley DE (1990). Some population genetic consequences of colony formation and extinction: genetic correlations within founding groups. *Evolution (N Y)* **44**: 1717–1724.

Wilson GA, Rannala B (2003). Bayesian inference of recent migration rates using multilocus genotypes. *Genetics* **163**: 1177–91.

DATA ACCESSIBILITY

Genotypes are available at Dryad doi:xxx

SUPPORTING INFORMATION

Additional supporting information may be found in the online version of this article:

Supplementary Table S1: Estimates of genetic diversity for each locus, for both species.

Supplementary Table S2: Estimates of contemporary gene flow among populations of *Viola tricolor* subsp. *curtisii*.

Supplementary Table S3: Estimates of contemporary gene flow among populations of *Crithmum maritimum.*

Supplementary Figure S1: Geographical distribution of genetic diversity in populations of *Crithmum maritimum.*

Supplementary Figure S2: Geographical distribution of genetic diversity in populations of *Viola tricolor* subsp. *curtisii*.

Supplementary Figure S3: sPCA results for *Crithmum maritimum.*

Supplementary Figure S4: Bayesian clustering of individuals of *Crithmum maritimum.*

Supplementary Figure S5: sPCA results for *Viola tricolor* subsp. *curtisii.*

Supplementary Figure S6: Bayesian clustering of individuals of *Viola tricolor* subsp. *curtisii.*

Supplementary Figure S7: Variation of the estimates of selfing rates along the geographic range, and covariation of the three estimates for *Crithmum maritimum.*

Supplementary Figure S8: Variation of the estimates of selfing rates along the geographic range, and covariation of the three estimates for *Viola tricolor* subsp. *curtisii*.